

Anisotropic photon emission from gluon fusion and splitting in a strong magnetic background: The two-gluon one-photon vertex

Alejandro Ayala ^{1,2,3} Jorge David Castaño-Yepes ⁴ L. A. Hernández ^{5,6} Ana Julia Mizher ^{7,8}
María Elena Tejada-Yeomans ^{9,10} and R. Zamora ^{11,12}

¹*Instituto de Ciencias Nucleares, Universidad Nacional Autónoma de México, Apartado Postal 70-543, CdMx 04510, Mexico*

²*Centre for Theoretical and Mathematical Physics, and Department of Physics, University of Cape Town, Rondebosch 7700, South Africa*

³*Departamento de Física, Universidade Federal de Santa Maria, Santa Maria, RS 97105-900, Brazil*

⁴*Instituto de Física, Pontificia Universidad Católica de Chile, Vicuña Mackenna 4860, Santiago, Chile*

⁵*Departamento de Física, Universidad Autónoma Metropolitana-Iztapalapa, Av. San Rafael Atlixco 186, C.P. CdMx 09340, Mexico*

⁶*Facultad de Ciencias de la Educación, Universidad Autónoma de Tlaxcala, Tlaxcala, 90000, Mexico*

⁷*Instituto de Física Teórica, Estadual Paulista, Rua Dr. Bento Teobaldo Ferraz, 271 - Bloco II, 01140-070 São Paulo, SP, Brazil*

⁸*Centro de Ciencias Exactas, Universidad del Bío-Bío, Avda. Andrés Bello 720, Casilla 447, 3800708, Chillán, Chile*

⁹*Facultad de Ciencias - CUICBAS, Universidad de Colima, Bernal Díaz del Castillo No. 340,*

Col. Villas San Sebastián, 28045 Colima, Mexico

¹⁰*Perimeter Institute for Theoretical Physics, 31 Caroline Street North Waterloo, Ontario N2L 2Y5, Canada*

¹¹*Instituto de Ciencias Básicas, Universidad Diego Portales, Casilla 298-V, Santiago, Chile*

¹²*Centro de Investigación y Desarrollo en Ciencias Aeroespaciales (CIDCA), Fuerza Aérea de Chile, Casilla 8020744, Santiago, Chile*



(Received 22 September 2022; accepted 30 November 2022; published 12 December 2022)

Having in mind the pre-equilibrium stage in peripheral heavy-ion collisions as a possible scenario for the production of electromagnetic radiation, we compute the two-gluon one-photon vertex in the presence of an intense magnetic field at one-loop order. The quarks in the loop are taken such that two of them occupy the lowest Landau level, with the third one occupying the first excited Landau level. When the field strength is the largest of the energy (squared) scales, the tensor basis describing this vertex corresponds to two of the three-vector particles polarized in the longitudinal direction whereas the third one is polarized in the transverse direction. However, when the photon energy is of the same order as or larger than the field strength, the explicit one-loop computation contains extra tensor structures that spoil the properties of the basis compared with the case when the field strength is the largest of the energy scales, which signals that the calculation is incomplete. Nevertheless, by projecting the result onto the would-be basis, we show that the squared amplitude for processes involving two gluons and one photon exhibits the expected properties such as a preferred in-plane photon emission and a slightly decreasing strength for an increasing magnetic-field strength. We comment on possible venues to improve the one-loop calculation that include accounting for progressive occupation of the three quarks of the lowest and first-excited Landau levels such that, still working in the large field limit, a more complete description can be achieved when the photon energy increases.

DOI: [10.1103/PhysRevC.106.064905](https://doi.org/10.1103/PhysRevC.106.064905)

I. INTRODUCTION

There are several intriguing properties associated with the direct photons produced in the aftermath of relativistic heavy-ion collisions. The first is the large magnitude of their elliptic flow coefficient v_2 , found to be similar to that of hadrons [1–3]. Since the latter comes mainly from the late stages of the collision, when flow is already built up, it may be thought

that direct photons are also preferably produced during the hadronic part of the system's evolution. However, the yields seemingly have a large thermal component that dominates over the prompt one for low values of the transverse momentum p_T . In fact, the low- p_T part of the spectrum is used to characterize the system's temperature which turns out to have large values that can originate only during the very early thermal history of the collision. The early emission of the bulk of the direct photons seems to be confirmed by the measured p_T dependence of v_2 which, for large p_T , is consistent with zero. This can be understood when considering that photons, being a penetrating probe, can only be boosted by conditions experienced at the times when they are produced. If they in fact come from the early stages, when velocities are small, their v_2 for large p_T should tend to zero [4], as observed. Put

Published by the American Physical Society under the terms of the Creative Commons Attribution 4.0 International license. Further distribution of this work must maintain attribution to the author(s) and the published article's title, journal citation, and DOI. Funded by SCOAP³.

together, these properties have been dubbed the *direct photon puzzle*.

In addition, an excess of low- p_T photons, with respect to known sources and even to descriptions that work well for other electromagnetic probes, has been found by PHENIX [5]. Their analyses show that the yield of these low- p_T photons scales with a given power of the number of binary collisions, both in Au + Au and Cu + Cu systems [6], which suggests that the source of these photons is similar for different colliding species and beam energies. However, it should be pointed out that a tension exists between the photon yields measured by the PHENIX and STAR Collaborations [7] and that, for the latter as well as for recent ALICE Collaboration measurements [8], the difference with state-of-the-art calculations for direct photon emission [9–11] is either not present or exists only within experimental uncertainties. Future photon measurements in a lower energy domain, such as the one to be carried out by the NICA-MPD experiment [12], promises to provide valuable complementary information.

Attempts to find possible missing contributions for the description of the photon yield have recently paid attention to the electromagnetic radiation produced during a pre-equilibrium stage. [13–16]. At early times, an anisotropy in the gluon distribution, caused by a possible anisotropy in the pressure, together with a delayed equilibration of the Glasma, may lead to an anisotropic photon emission [17]. A momentum-anisotropic quark-gluon plasma (QGP), with a hydrodynamic evolution of the momentum distributions from the initial stage, may also contribute to photon emission and have a noticeable impact on v_2 for intermediate and large p_T [18].

Another source of extra electromagnetic radiation, that at the same time provides a natural anisotropic emission, is the presence of a magnetic field. A magnetic field provides not only a direction that breaks rotational invariance and can be a source of v_2 but it also opens new channels for photon emission. For instance, in a quark-gluon plasma, photons can be emitted by magnetic-field-induced bremsstrahlung and pair annihilation [19–22]. The closely related dilepton production processes in a magnetized QGP has also been addressed in Refs. [23,24]. The QED \times QCD conformal anomaly [25] or fluctuations of the gluon coupled to the photon stress tensor [26] can be a source of soft photons as well. Holography has also been employed to describe photon production from a strongly coupled plasma in the presence of intense magnetic fields [27–30].

Recall that magnetic fields of a sizable intensity may be produced in semicentral heavy-ion collisions [31–35]. Although the intensity of the field generated by spectators drops very fast, which causes an incomplete electromagnetic response in the medium formed at later times [36,37], the field is found to be very intense during pre-equilibrium. Recent experimental results corroborate earlier theoretical predictions indicating a peak value $B \approx 10^{19}$ G for energies of the BNL Relativistic Heavy Ion Collider (RHIC) [38,39]. Experimental analyses aiming to characterize the time evolution of the field are on its way.

In a couple of recent works [40,41] we have put forward the idea that the presence of a magnetic field in the

pre-equilibrium stage of the heavy-ion collision opens the gluon fusion and splitting channels for photon production. According to the bottom-up thermalization evolution scenario [42] during this stage, nonequilibrium distributions of quarks and gluons, f_q and f_g , respectively, describe the particle occupation numbers, with quarks being suppressed with respect to gluons by the relation $f_q \sim \alpha_s f_g$ [43,44]. Although the quark or antiquark splitting and quark-antiquark annihilation amplitudes represent the leading perturbative matrix element for photon emission, overall at pre-equilibrium, this process is suppressed by a factor α_s^2 . If one accounts for Pauli blocking in the final state, the suppression for low energy photon emission is even larger making gluon fusion or splitting to be comparable in intensity to the former processes. As a consequence, gluon fusion or splitting, together with the large abundance of soft pre-equilibrium gluons, contribute to enhance the photon yield and v_2 . In Refs. [40,41] a drastic approximation whereby the field intensity is taken as the largest energy (squared) scale was employed. This approximation limits the accuracy of the results to the very-low- p_T part of the spectra. In this work we relax this approximation and do not set such restriction between the magnitude of the photon p_T^2 and the field intensity, although we still work in the strong-field limit as compared with the square of the masses of the active quark species. Given the complexity of the calculation, here we limit ourselves to computing the one-loop two-gluon one-photon vertex that describes this process and reserve the application of its contribution to the photon yield and v_2 for a follow-up work. It is worth mentioning that the techniques used in Refs. [40,41], have also influenced recent treatments to obtain the corrections to the anomalous magnetic moment of the electron or muon and the corresponding ones of the anomalous magnetic moment of quarks, in the presence of a magnetic field with a strength comparable to the fermion masses [45,46].

The work is organized as follows: In Sec. II we set up the ingredients to compute the vertex function describing the on-shell coupling between two gluons and a photon in the presence of a magnetic field. In the strong-field limit, we spell out the most general expression for this vertex consistent with parity, charge conjugation and gauge invariance. In Sec. III, we explicitly compute the one-loop contribution to the vertex function in the presence of a magnetic field. We make use of the Landau-level representation of the quark propagators and work in the strong-field limit, with the quarks occupying the lowest possible Landau levels that produce a nonvanishing result. This requires that two of the quarks are in the lowest Landau level (LLL) and the other in the first-excited Landau levels (1LL). To extend the work of Refs. [40,41], where the calculations were performed in the large-field limit and neglecting the momentum in the quark line occupying the 1LL, here we remove the latter simplifying assumption. We explicitly compute the coefficients for the tensor basis that describe the matrix element and show that, when the photon energy squared is allowed to be comparable to the magnetic-field strength, the explicit one-loop calculation contains extra terms not present in the basis corresponding to the case where the magnetic-field strength dominates the energy scales of the problem. We finally summarize and provide an outlook of the

calculation to set a possible route to avoid these shortcomings in Sec. IV.

II. TWO-GLUON ONE-PHOTON VERTEX IN A MAGNETIC BACKGROUND

The coupling between two gluons and one photon is made possible by the presence of the external magnetic field. According to Furry's theorem, the coupling vanishes in the absence of this field since both QED and QCD are charge-conjugation-conserving theories. The breaking of Lorentz invariance, also induced by the magnetic field, separates space-time into parallel and perpendicular pieces with respect to the magnetic field. For definiteness, let us consider a constant in time and spatially uniform magnetic field of strength B pointing along the \hat{z} direction. The separation of space-time is implemented by introducing the tensor metric components such that [47]

$$g^{\mu\nu} = g_{\parallel}^{\mu\nu} + g_{\perp}^{\mu\nu}, \quad (1a)$$

$$g_{\parallel}^{\mu\nu} = \text{diag}(1, 0, 0, -1),$$

$$g_{\perp}^{\mu\nu} = \text{diag}(0, -1, -1, 0), \quad (1b)$$

which implies that, for any four-vector p^{μ} , we can write

$$p_{\parallel}^{\mu} = (p_0, 0, 0, p_3), \quad (2a)$$

$$p_{\perp}^{\mu} = (0, p_1, p_2, 0),$$

and

$$p^2 = p_{\parallel}^2 - p_{\perp}^2, \quad (2b)$$

where $p_{\parallel}^2 \equiv p_0^2 - p_3^2$ and $p_{\perp}^2 = p_1^2 + p_2^2$. Therefore, the most general tensor structure for a third-rank tensor, such as the two-gluon one-photon vertex $\Gamma_{ab}^{\mu\nu\alpha}$, where μ, ν, α and a, b are Lorentz and color indices, respectively, involves the metric tensors in the parallel and perpendicular directions,

$$g_{\parallel}^{\mu\nu}, \quad g_{\perp}^{\mu\nu}, \quad (3)$$

and the momentum components of the gluons and the photon, also in the parallel and perpendicular directions, namely,

$$p_{\parallel}^{\alpha}, \quad p_{\perp}^{\alpha}, \quad k_{\parallel}^{\alpha}, \quad k_{\perp}^{\alpha}, \quad q_{\parallel}^{\alpha}, \quad q_{\perp}^{\alpha}, \quad (4)$$

where p, k , and q are the four-momenta of the gluons and of the photon, respectively.

The kind of magnetic field hereby considered cannot transfer energy-momentum to the gluons and the photon. Thus, when also neglecting possibly medium-induced modification on their dispersion properties, energy-momentum conservation imposes that, for on-shell propagation, all the four-momenta are parallel [48]

$$q^{\mu} = p^{\mu} + k^{\mu}. \quad (5)$$

Choosing q^{μ} as the reference four-momentum, we have

$$p^{\mu} = \left(\frac{\omega_p}{\omega_q}\right) q^{\mu}, \quad (6a)$$

$$k^{\mu} = \left(\frac{\omega_k}{\omega_q}\right) q^{\mu}, \quad (6b)$$

where $\omega_p, \omega_k, \omega_q$ are the energies of the gluons and photon, respectively. The on-shell restriction implies a reduction of the tensor structures involved in the vertex construction. Then, it is enough to consider tensors obtained from the combination of

$$g_{\parallel}^{\mu\nu}, \quad g_{\perp}^{\mu\nu}, \quad q_{\parallel}^{\alpha}, \quad q_{\perp}^{\alpha}. \quad (7)$$

Following the findings of Refs. [40,41], in the approximation where the magnetic field is the largest of the kinematical energy (squared) variables, the tensor structure can be expressed as

$$\begin{aligned} \Gamma_{ab}^{\mu\nu\alpha} &= \delta_{ab} \Gamma^{\mu\nu\alpha}, \\ \Gamma^{\mu\nu\alpha} &\equiv \Gamma_1(\omega_q, \omega_k, q^2) \frac{\epsilon_{ij} q_{\perp}^i g_{\perp}^{j\mu}}{\sqrt{q_{\perp}^2}} \left(g_{\parallel}^{\nu\alpha} - \frac{q_{\parallel}^{\nu} q_{\parallel}^{\alpha}}{q_{\parallel}^2} \right) \\ &+ \Gamma_2(\omega_q, \omega_k, q^2) \frac{\epsilon_{ij} q_{\perp}^i g_{\perp}^{j\nu}}{\sqrt{q_{\perp}^2}} \left(g_{\parallel}^{\mu\alpha} - \frac{q_{\parallel}^{\mu} q_{\parallel}^{\alpha}}{q_{\parallel}^2} \right) \\ &+ \Gamma_3(\omega_q, \omega_k, q^2) \frac{\epsilon_{ij} q_{\perp}^i g_{\perp}^{j\alpha}}{\sqrt{q_{\perp}^2}} \left(g_{\parallel}^{\mu\nu} - \frac{q_{\parallel}^{\mu} q_{\parallel}^{\nu}}{q_{\parallel}^2} \right) \\ &\equiv \sum_{n=1}^3 \Gamma_n(\omega_q, \omega_k, q^2) \Gamma_n^{\mu\nu\alpha}, \end{aligned} \quad (8)$$

where $\Gamma_n(\omega_q, \omega_k, q^2)$, $n = 1, 2, 3$, are scalar coefficients and ϵ_{ij} is the Levy-Civita symbol in the transverse components: $\epsilon_{12} = -\epsilon_{21} = 1$. Since $q^2 = 0$, we can use either q_{\parallel}^2 or q_{\perp}^2 to describe the functional dependence of the coefficients Γ_n on the photon's momentum. Notice that

$$v_{\perp}^{\beta} \equiv \epsilon_{ij} \frac{q_{\perp}^i g_{\perp}^{j\beta}}{\sqrt{q_{\perp}^2}} \quad (9)$$

corresponds to the polarization vector for transverse (with respect to the magnetic field) modes and also that in the strong-field limit, two of the three particles, either one of the gluons and the photon or the two gluons, propagate in the parallel polarization mode, characterized by a vector v_{\parallel}^{σ} that satisfies [49]

$$v_{\parallel}^{\sigma} v_{\parallel}^{\rho} \equiv \Pi_{\parallel}^{\sigma\rho} = g_{\parallel}^{\sigma\rho} - \frac{q_{\parallel}^{\sigma} q_{\parallel}^{\rho}}{q_{\parallel}^2}. \quad (10)$$

The tensor basis of Eq. (8) is orthonormal, namely,

$$\Gamma_n^{\sigma\rho\beta} \Gamma_{\sigma\rho\beta m} = \delta_{nm}. \quad (11)$$

This basis is also complete, when the magnetic field can be taken as the largest possible energy (squared). Relaxing this condition introduces extra terms in the basis whose importance increases as the ratio $\omega_q^2/|eB|$ increases. In the strong-field approximation, the physical picture that emerges is as follows: It is well known that a strong magnetic field forces two of the vector particles to occupy parallel polarization states [47,50,51]. When the vertex involves a third vector particle, invariance under charge conjugation and conservation of angular momentum require that its polarization state

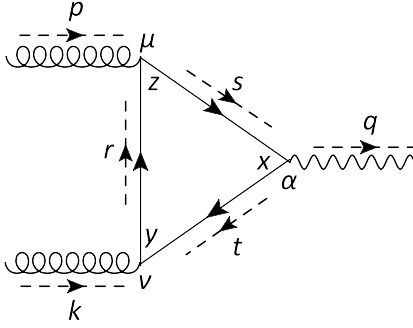


FIG. 1. Feynman diagram describing the coupling between two gluons and a photon at lowest order in α_s and α_{em} in the presence of a magnetic field.

is transverse. At the lowest perturbative order, this can be understood recalling that, when polarized in the same direction, the addition of the three spin 1/2 quarks in the loop gives rise to a half-integer spin state that cannot describe the spin state of a combination of three-vector particles. Therefore, one of the quarks that make up the loop needs to be placed not in the LLL but instead in the 1LL. This in turn induces the emergence of a transverse mode to be occupied by one of the vector particles. Similar selection rules, albeit in the weak-field limit, are discussed in Ref. [48].

Parity conservation requires that the vertex is symmetric under the exchange of the gluon Lorentz indices $\mu \leftrightarrow \nu$, which in turn requires that, when $\omega_p \leftrightarrow \omega_k$, $\Gamma_1 \leftrightarrow \Gamma_2$, while Γ_3 remains invariant. The vertex also satisfies the transversality condition

$$q_\mu \Gamma^{\mu\nu\alpha} = q_\nu \Gamma^{\mu\nu\alpha} = q_\alpha \Gamma^{\mu\nu\alpha} = 0 \quad (12)$$

imposed by gauge invariance. Relaxing the strong-field approximation to partially account for contributions to allow that the photon energy (squared) is not small compared with the magnetic-field intensity spoils the symmetry properties. We explicitly show this in the following section, where we compute the coefficients Γ_n at leading order in the strong magnetic field at the one-loop level. This calculation provides the key features of photon production in the kinematical regions of interest in the context of the *direct photon puzzle* and sheds light on the road to improve the approximation.

III. ONE-LOOP VERTEX IN THE STRONG-FIELD LIMIT

The scattering process involving two gluons and a photon, either gluon fusion or splitting, is described at leading order in the strong, $\alpha_s = g^2/4\pi$, and electromagnetic, $\alpha_{em} = e^2/4\pi$, couplings by a Feynman diagram that is represented as a fermion triangle with two gluons and one photon attached to the vertices. Given that the magnetic field breaks Lorentz symmetry, the vertex describing these processes needs to be computed starting from configuration space. Figure 1 shows the generic diagram where the internal lines correspond to fermion propagators in the presence of a magnetic field, which

can be written as

$$S(x, x') = \Phi(x, x') \int \frac{d^4 p}{(2\pi)^4} e^{-ip \cdot (x-x')} S(p), \quad (13)$$

where $\Phi(x, x')$ is Schwinger's phase factor that, for a fermion with charge q_f , is given by

$$\Phi(x, x') = \exp \left\{ iq_f \int_{x'}^x d\xi^\mu \left[A^\mu + \frac{1}{2} F_{\mu\nu} (\xi - x')^\nu \right] \right\}. \quad (14)$$

The Fourier transform of the translationally invariant part of the propagator can be expressed as a sum over Landau levels such that

$$iS(p) = ie^{-p_\perp^2/|q_f B|} \sum_{n=0}^{+\infty} \frac{(-1)^n D_n(|q_f B|, p)}{p_\parallel^2 - m_f^2 - 2n|q_f B| + i\epsilon}, \quad (15)$$

with m_f being the fermion mass and

$$\begin{aligned} D_n(|q_f B|, p) = & 2(\not{p}_\parallel + m_f) \mathcal{O}^- L_n^0 \left(\frac{2p_\perp^2}{|q_f B|} \right) \\ & - 2(\not{p}_\parallel + m_f) \mathcal{O}^+ L_{n-1}^0 \left(\frac{2p_\perp^2}{|q_f B|} \right) \\ & + 4\not{p}_\perp L_{n-1}^1 \left(\frac{2p_\perp^2}{|q_f B|} \right), \end{aligned} \quad (16)$$

where $L_n^m(x)$ are the generalized Laguerre polynomials, and the operators \mathcal{O}^\pm are given by

$$\mathcal{O}^\pm = \frac{1}{2} [1 \pm i\gamma^1 \gamma^2 \text{sign}(q_f B)]. \quad (17)$$

From the Feynman diagram of Fig. 1, we write the expression for the vertex as

$$\begin{aligned} \Gamma_{\mu\nu\alpha}^{ab} = & - \int d^4 x d^4 y d^4 z \int \frac{d^4 r}{(2\pi)^4} \frac{d^4 s}{(2\pi)^4} \frac{d^4 t}{(2\pi)^4} \\ & \times e^{-it \cdot (y-x)} e^{-is \cdot (x-z)} e^{-ir \cdot (z-y)} e^{-ip \cdot z} e^{-ik \cdot y} e^{iq \cdot x} \\ & \times \{ \text{Tr}[iq_f \gamma_\alpha iS(s) ig\gamma_\mu t^a iS(r) ig\gamma_\nu t^b iS(t)] \\ & + \text{Tr}[iq_f \gamma_\alpha iS(t) ig\gamma_\nu t^b iS(r) ig\gamma_\mu t^a iS(s)] \} \\ & \times \Phi(x, y) \Phi(y, z) \Phi(z, x), \end{aligned} \quad (18)$$

where p and k are the gluon and q are the photon four-momenta, $t^a = \lambda^a/2$, $t^b = \lambda^b/2$ with λ^a and λ^b being Gell-Mann matrices. Notice that, in the last equation, the contribution from the charge-conjugate diagram is also considered.

To describe a constant magnetic field that points in the z direction, the vector potential A^μ can be chosen in the symmetric gauge,

$$A^\mu = \frac{B}{2} (0, -y, x, 0), \quad (19)$$

so that, from Eq. (14), the product of Schwinger phases is given by

$$\Phi(x, y) \Phi(y, z) \Phi(z, x) = e^{-i \frac{|q_f B|}{2} \epsilon_{m_j} (z-x)_m (x-y)_j}, \quad (20)$$

where the indices $m, j = 1, 2$. It has been shown that when considering localized interactions, such as in the present calculation, the product of Schwinger phases is gauge invariant [52].

Given that at the early stages of a heavy-ion collision the magnetic field is at its peak intensity, we can work in the strong-field approximation, whereby fermions in the loop occupy the lowest possible Landau levels, and one takes

$|q_f B| \gg m_f^2$. In Refs. [40,41], it has been shown that the first-order nonvanishing contribution in the large-field limit requires two of the fermion propagators to occupy the LLL whereas the third one occupies the 1LL, which correspond to $n = 0$ and $n = 1$ in Eq. (15), respectively:

$$iS_{\text{LLL}}(p) = i \frac{e^{-p_{\perp}^2/q_f B}}{p_{\parallel}^2 - m_f^2 + i\epsilon} (\not{p}_{\parallel} + m_f) \mathcal{O}^-, \quad (21)$$

$$iS_{\text{1LL}}(p) = -2i \frac{e^{-p_{\perp}^2/q_f B}}{p_{\parallel}^2 - m_f^2 - 2|q_f B| + i\epsilon} \left[(\not{p}_{\parallel} + m_f) \left(1 - \frac{2p_{\perp}^2}{|q_f B|} \right) \mathcal{O}^- - (\not{p}_{\parallel} + m_f) \mathcal{O}^+ + 2\not{p}_{\perp} \right]. \quad (22)$$

The contributing Feynman diagrams, obtained when placing two fermion propagators in the LLL and the other in the 1LL, are depicted in Fig. 2. After integration of the configuration space variables, the vertex in Eq. (18) is given by

$$\Gamma_{ab}^{\mu\nu\alpha} = -\delta^{(4)}(q - k - p) \text{Tr}[t_a t_b] \frac{8\pi^4 q_f g^2}{|q_f B|} q_{\parallel}^2 e^{f(p_{\perp}, k_{\perp})} \sum_{i=1}^3 D_i^{\mu\nu\alpha}, \quad (23)$$

where

$$f(p_{\perp}, k_{\perp}) = \frac{1}{8|q_f B|} [p_m - k_m + i\epsilon_{mj}(p_j + k_j)]^2 \frac{1}{2|q_f B|} (p_m^2 + k_m^2 + 2i\epsilon_{jm} p_m k_j) \quad (24)$$

and

$$D_1^{\mu\nu\alpha} = \left\{ 2|q_{\perp}| \mathcal{I}_1 \left[(\tilde{C} v_{\perp}^{\nu} + i q_{\perp}^{\nu}) \left(\Pi_{\parallel}^{\mu\alpha} - \frac{1}{2} g_{\parallel}^{\mu\alpha} \right) - (\tilde{C} v_{\perp}^{\mu} + i q_{\perp}^{\mu}) \left(\Pi_{\parallel}^{\nu\alpha} - \frac{1}{2} g_{\parallel}^{\nu\alpha} \right) \right] + 2\mathcal{J}_1 \epsilon_{ij} g_{\perp}^{i\mu} g_{\perp}^{j\nu} q_{\parallel}^{\alpha} \right\}, \quad (25)$$

$$D_2^{\mu\nu\alpha} = \left\{ 2|q_{\perp}| \mathcal{I}_2 \left[\left(\tilde{B} v_{\perp}^{\mu} + \frac{3i\omega_k}{4\omega_q} q_{\perp}^{\mu} \right) \left(\Pi_{\parallel}^{\nu\alpha} - \frac{1}{2} g_{\parallel}^{\nu\alpha} \right) - \left(\tilde{B} v_{\perp}^{\nu} + \frac{3i\omega_k}{4\omega_q} q_{\perp}^{\nu} \right) \left(\Pi_{\parallel}^{\mu\alpha} - \frac{1}{2} g_{\parallel}^{\mu\alpha} \right) \right] + 2\mathcal{J}_2 \epsilon_{ij} g_{\perp}^{i\alpha} g_{\perp}^{j\mu} q_{\parallel}^{\nu} \right\}, \quad (26)$$

$$D_3^{\mu\nu\alpha} = \left\{ 2\mathcal{I}_3 \left[(-i\tilde{A}_1 q_{\perp}^{\nu} - \tilde{A}_2 |q_{\perp}| v_{\perp}^{\nu}) \left(\Pi_{\parallel}^{\mu\alpha} - \frac{1}{2} g_{\parallel}^{\mu\alpha} \right) + (i\tilde{A}_1 q_{\perp}^{\mu} + \tilde{A}_2 |q_{\perp}| v_{\perp}^{\mu}) \left(\Pi_{\parallel}^{\nu\alpha} - \frac{1}{2} g_{\parallel}^{\nu\alpha} \right) \right] + 2\mathcal{J}_3 \epsilon_{ij} g_{\perp}^{i\nu} g_{\perp}^{j\alpha} q_{\parallel}^{\mu} \right\}, \quad (27)$$

with the coefficients \tilde{A} , \tilde{B} , and \tilde{C} given by

$$\tilde{A}_1(\omega_k, \omega_q) \equiv -\frac{\tilde{C}}{8} - \frac{\omega_p}{\omega_q} - \frac{1}{8}, \quad (28a)$$

$$\tilde{A}_2(\omega_k, \omega_q) \equiv -\frac{\tilde{C}}{8} + \frac{\omega_k}{2\omega_q} + \frac{1}{4}, \quad (28b)$$

$$\tilde{B} \equiv \frac{2\omega_k - 3\omega_q}{\omega_q} + \frac{i}{2}, \quad (28c)$$

$$\tilde{C} \equiv \frac{\omega_p - \omega_k}{\omega_q}, \quad (28d)$$

and where we have defined

$$\mathcal{I}_1 \equiv \int_0^1 dx \int_0^{1-x} dy \frac{x + \frac{\omega_k}{\omega_q}(1-x-y) - [x + \frac{\omega_k}{\omega_q}(1-x-y)]^2}{\Delta_1^2(x, y)}, \quad (29a)$$

$$\begin{aligned} \mathcal{J}_1 \equiv & \int_0^1 dx \int_0^{1-x} dy \left[\frac{2x + 2(1-x-y)\frac{\omega_k}{\omega_q} - 1}{\Delta_1(x, y) q_{\parallel}^2} + \frac{1}{\Delta_1^2(x, y)} \left\{ \left[\left(x + \frac{\omega_k}{\omega_q}(1-x-y) \right)^2 \right. \right. \right. \\ & - \left. \left(x + (1-x-y)\frac{\omega_k}{\omega_q} \right) \frac{\omega_k}{\omega_q} \right] + \left(x + (1-x-y)\frac{\omega_k}{\omega_q} \right) \frac{\omega_k(\omega_q - \omega_k)}{\omega_q^2} - \left[\left(x + (1-x-y)\frac{\omega_k}{\omega_q} \right)^2 \right. \\ & \left. \left. + \left(1 - 2x - 2(1-x-y)\frac{\omega_k}{\omega_q} \right) \frac{\omega_k}{\omega_q} \right] \left(x + (1-x-y)\frac{\omega_k}{\omega_q} \right) \right\} \right], \quad (29b) \end{aligned}$$

$$\Delta_1(x, y) = [x + (1 - x - y)(\omega_k/\omega_q)]^2 q_{\parallel}^2 - xq_{\parallel}^2 - (1 - x - y)[(\omega_k/\omega_q)^2 q_{\parallel}^2 - 2|q_f B|] + m_f^2, \quad (29c)$$

$$\mathcal{I}_2 \equiv \int_0^1 dx \int_0^{1-x} dy \frac{[(\frac{\omega_k}{\omega_q}x + (1 - x - y))^2 - \frac{\omega_k}{\omega_q}(\frac{\omega_k}{\omega_q}x + (1 - x - y))]}{\Delta_2^2(x, y)}, \quad (30a)$$

$$\begin{aligned} \mathcal{J}_2 \equiv \int_0^1 dx \int_0^{1-x} dy & \left[\frac{(1 - 2x)\frac{\omega_k}{\omega_q} - 2(1 - x - y)}{\Delta_2(x, y)q_{\parallel}^2} + \frac{1}{\Delta_2^2(x, y)} \left\{ \left[\left((1 - x - y) - \frac{\omega_k}{\omega_q}x \right) \frac{\omega_k}{\omega_q} \right. \right. \right. \\ & - \left. \left. \left((1 - x - y) + \frac{\omega_k}{\omega_q}x \right)^2 \right] + \left((1 - x - y) + \frac{\omega_k}{\omega_q}x \right) \frac{\omega_k(\omega_q - \omega_k)}{\omega_q^2} + \left[\left((1 - x - y) + \frac{\omega_k}{\omega_q}x \right)^2 \right. \right. \\ & \left. \left. - \left(2x - 1 + 2(1 - x - y)\frac{\omega_k}{\omega_q} \right) \frac{\omega_k}{\omega_q} \right] \left((1 - x - y) + \frac{\omega_k}{\omega_q}x \right) \right\} \right], \quad (30b) \end{aligned}$$

$$\Delta_2(x, y) = [(1 - x - y) + (\omega_k/\omega_q)x]^2 q_{\parallel}^2 - x(\omega_k/\omega_q)^2 q_{\parallel}^2 - (1 - x - y)(q_{\parallel}^2 - 2|q_f B|) + m_f^2, \quad (30c)$$

$$\mathcal{I}_3 \equiv \int_0^1 dx \int_0^{1-x} dy \frac{-x + \frac{\omega_k}{\omega_q}[y - \frac{\omega_k}{\omega_q}(1 - x - y)] + [x + \frac{\omega_k}{\omega_q}(1 - x - y)]^2}{\Delta_3^2(x, y)}, \quad (31)$$

$$\mathcal{J}_3 \equiv \int_0^1 dx \int_0^{1-x} dy \frac{-i}{8\pi} \frac{1}{\Delta_3^2} \left[\left(\frac{\omega_p + 2\omega_k}{\omega_q} \right) \Delta_3 + \left[\tilde{f}^3 - \tilde{f}^2 \left(1 + \frac{\omega_k}{\omega_q} \right) + \tilde{f} \frac{\omega_k}{\omega_q} \right] q_{\parallel}^2 \right], \quad (32)$$

$$\Delta_3(x, y) = \left[x + (1 - x - y)\frac{\omega_k}{\omega_q} \right]^2 q_{\parallel}^2 - xq_{\parallel}^2 - (1 - x - y)k_{\parallel}^2 + 2|q_f B|y + m_f^2, \quad (33)$$

with

$$\tilde{f} \equiv x + (1 - x - y)\frac{\omega_k}{\omega_q}. \quad (34)$$

We emphasize that Eqs. (25)–(27) are obtained under the approximation whereby $|q_f B| \gg m_f^2$ in the numerator of Eqs. (21) and (22). This is a reasonable approximation when accounting only for the active quark species u, d, s and during the pre-equilibrium and/or very early stages of the collision. On the other hand, the masses in the denominator need to be kept finite so that the integrand is infrared safe. This is explicitly shown in Appendix A.

To perform the integrals, we implement a Wick rotation in the q_0 component of the photon momentum, namely,

$$q_0^2 = \omega_q^2 \rightarrow -(q_0^E)^2. \quad (35)$$

Since the integrals to perform are written in terms of q_{\parallel}^2 , we need to keep track of the consequences of this Wick rotation to then come back by means of an analytical continuation to Minkowski space. The parallel component of the four-momentum transforms under this Wick rotation as

$$\begin{aligned} q_{\parallel}^2 & \rightarrow -\left[(q_0^E)^2 + q_3^2 \right] \equiv -(q_{\parallel}^E)^2 \\ & = -\omega_q^2(1 + \cos^2 \theta), \quad (36) \end{aligned}$$

where θ is the angle between the photon's direction of motion and the magnetic-field direction, namely, the \hat{z} axis. Thus, after integrating over the Feynman parameters x and y , we can analytically continue back to Minkowski space by replacing

$$(q_{\parallel}^E)^2 \rightarrow \omega_q^2(1 - \cos^2 \theta) = \omega_q^2 \sin^2 \theta. \quad (37)$$

In Appendix (B) we calculate $\Gamma_n(\omega_q, \omega_k, q^2)$ for $n = 1, 2, 3$ in Eq. (8), by projecting Eq. (23) onto a basis, where we have used both the transverse polarization vector and the longitudinal polarization tensor as defined in Eqs. (9) and (10). The functions Γ_i have real and imaginary parts and are defined in Eqs. (B5)–(B7) as

$$\Gamma_n \equiv \frac{8\pi^4 q_f g^2}{|q_f B|} e^{f(p_{\perp}, k_{\perp})} |q_{\perp}| \tilde{\Gamma}_n(\omega_q, \omega_k, \theta), \quad (38)$$

where we follow through on energy conservation as $\omega_q = \omega_p + \omega_k$. Figure 3 shows the sum of squared amplitudes $|\tilde{\Gamma}_n|$ as a function of the ratio of the photon energy to the quark mass for a fixed field strength and the full range of photon directions of propagation [Fig. 3(a)]; again as a function of the ratio of the photon energy to the quark mass for a fixed angle of the photon propagation with respect to the magnetic field direction, for a range of field strengths [Fig. 3(b)]; and as a function of the ratio of the photon energy (referred to a gluon energy) to the field strength, for a fixed value of the photon's direction of propagation, for different field intensities [Fig. 3(c)]. Notice that the sum of the squared amplitudes $|\tilde{\Gamma}_n|$ is larger for a photon propagation within the reaction plane

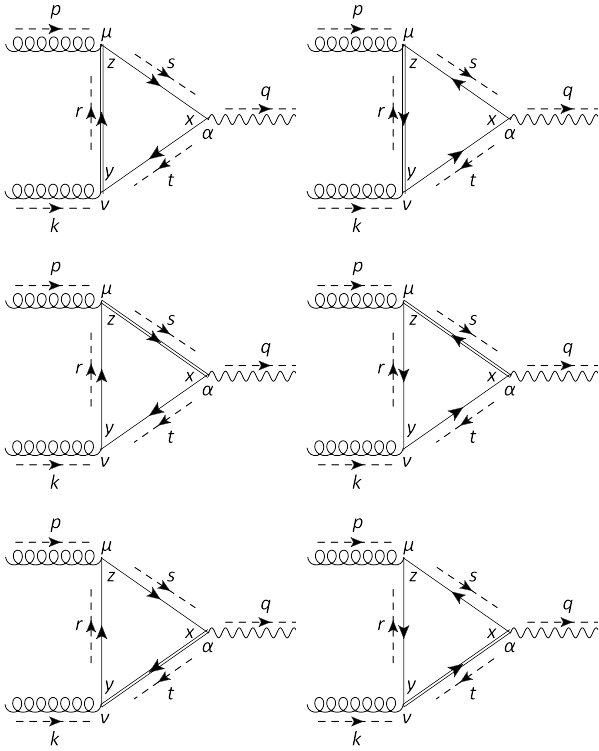


FIG. 2. Leading-order Feynman diagrams describing the vertex coupling two gluons and one photon in the presence of a magnetic field. The single lines represent fermion propagators in the lowest Landau level, and the double lines are propagators in the first-excited Landau level. The continuous and dashed arrows represent the flow of charge and momentum, respectively.

($\theta = \pi/2$) and that for $\theta = \pi/2$ it is also larger for smaller field intensities. On the other hand, notice that the prefactor $|q_{\perp}|e^{f(p_{\perp}, k_{\perp})}$ also depends on θ . Figure 4 shows this depen-

dence for different ω_k and $|q_f B|$ values for a range of fixed ratios ω_q/ω_k , [Fig. 4(a)] $\omega_k = 1$ GeV, $|q_f B| = m_{\pi}^2$; [Fig. 4(b)] $\omega_k = 1$ GeV, $|q_f B| = 5m_{\pi}^2$; and [Fig. 4(c)] $\omega_k = 0.1$ GeV, $|q_f B| = m_{\pi}^2$. Notice that the prefactor peaks at small angles for large gluon energies. In this case the squared amplitude is highly suppressed for angles close to the reaction plane. However, for small gluon energies and/or a large field strength, the prefactor is dominated by emission angles close to the reaction plane. Since at pre-equilibrium the largest gluon abundance happens for small energies, a positive v_2 coefficient may be expected. Last but not least, notice that the prefactor vanishes for $\theta = 0$, which prevents photons from being emitted along the direction of the magnetic field.

IV. SUMMARY AND OUTLOOK

In this work we have studied the two-gluon one-photon vertex induced by the presence of a magnetic field. The relevant physical scenario is the pre-equilibrium stage after a heavy-ion collision where the largest field intensities are achieved. During this stage, gluons are coupled to photons by means of virtual quarks and thus the former indirectly experience the influence of the field by the interaction of this with the latter. In this sense, arguments based on the suppression of the production of electromagnetic radiation at pre-equilibrium, due to the lack of quarks [36], do not apply when this radiation involves processes mediated by virtual quarks. The vertex for on-shell gluons and a photon can be constructed by multiplying the longitudinal polarization tensor, that describes the polarization of two of these vector particles, times a third polarization vector which is required to have components in the transverse plane, with respect to the magnetic field, the largest energy (squared) scale. However, when the photon energy squared is allowed to be on the order of or larger than the magnetic-field strength, this simple structure is spoiled. Nevertheless, in order to explore the bowels of this very complicated calculation,

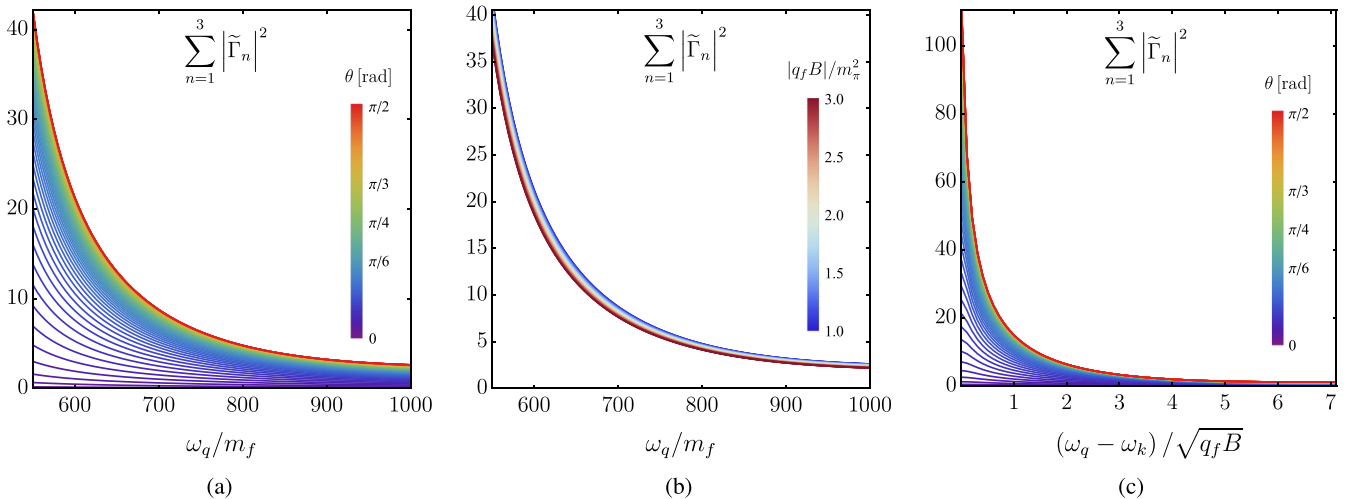


FIG. 3. Sum of squared amplitudes of $\tilde{\Gamma}_n$, $n = 1, 2, 3$ from Eqs. (B5)–(B7), as a function of (a) the photon energy ω_q and the angle with respect to the magnetic field θ with $|q_f B| = m_{\pi}^2$, (b) the photon energy ω_q and the magnetic field strength $|q_f B|$ with $\theta = \pi/2$, and (c) the ratio $(\omega_q - \omega_k)/\sqrt{|q_f B|}$ and the angle with respect to the magnetic field θ with $|q_f B| = m_{\pi}^2$. All the physical parameters are normalized by the quark mass $m_f = 2 \times 10^{-3}$ GeV, having fixed $\omega_k = 1$ GeV.

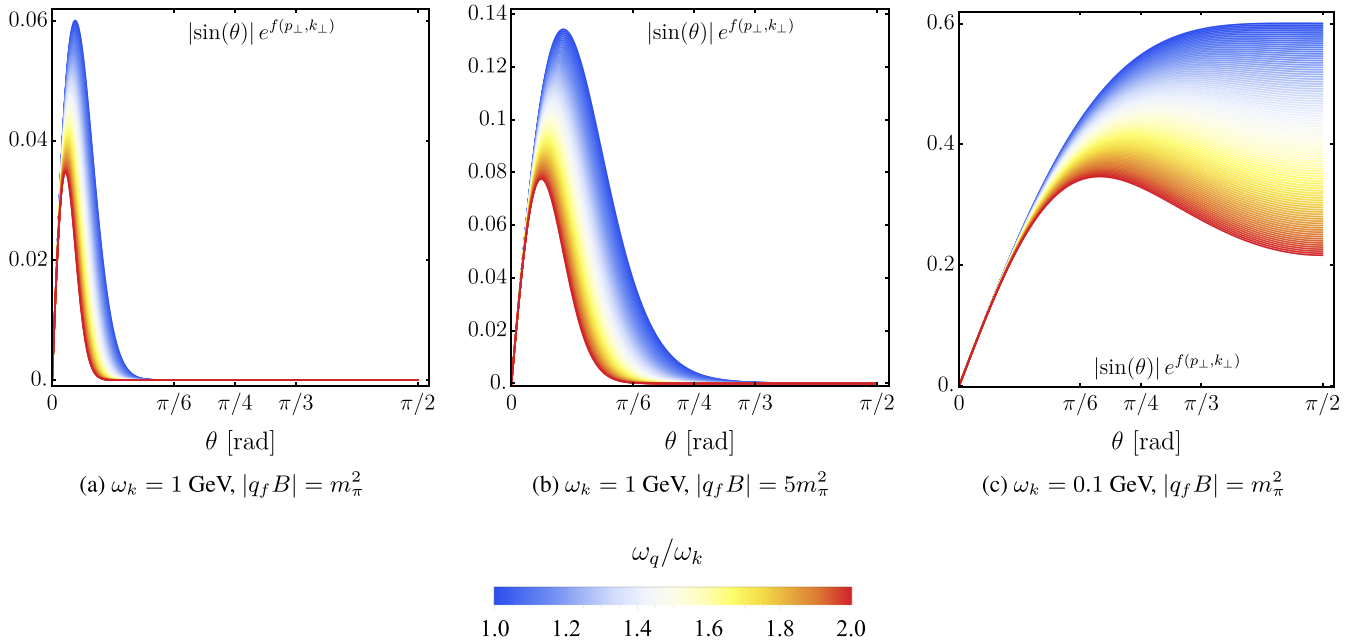


FIG. 4. Angular dependence of the factor $|q_{\perp}|e^{f(p_{\perp}, k_{\perp})}$ of Eq. (38) as a function of the photon's energy ω_q and the angle with respect to the magnetic field θ for fixed values of ω_k and $|q_f B|$.

we have computed the one-loop contribution, following the strategy of Refs. [40,41] applicable in the large-field limit. This consists of explicitly computing the one-loop contribution, placing two of the loop quarks in the LLL and the other one in the 1LL. The reason we worked with this configuration is that this represents the first nonvanishing contribution when quarks occupy progressive Landau levels starting from the lowest one, given that when all the quarks are in the LLL, the amplitude vanishes identically. When in the quark line occupying the 1LL the magnitude of the corresponding momentum squared is neglected with respect the magnetic-field intensity, the vertex turns out to respect the Ward identity and thus be made out of transverse tensor structures. In the present calculation we aimed at relaxing this approximation while keeping the form of the vertex and only allowing for the momentum in the corresponding quark line not to be neglected with respect to the field intensity. This is born from the observation that such approximation limits the accuracy of the results to the very-low- p_T part of the spectrum. It turns out that the explicit one-loop calculation with this extension introduces additional tensor structures for the vertex and thus that the use of the simple vertex to express these contributions is not enough. The extra structures do not respect the transversality nor the symmetry requirements for the vertex, signaling the incompleteness of the calculation. Nevertheless, with this procedure we have identified that allowing for the full momentum dependence of the quark line in the LLL requires the general structure of the vertex to be extended. At the same time one needs to consider at least all the possible Landau levels up to the first one for each of the quark lines in the one-loop calculation. To avoid these shortcomings, we are currently exploring the possibility to add one-loop corrections

where two and up to the three quarks in the loop occupy the 1LL. Our goal is to not only compute the vertex but also the corresponding rate for photon emission when using the appropriate gluon distribution function at pre-equilibrium and to compare our results to other nonequilibrium scenarios for photon production [13–16,43,44]. Needless to say this calculation is very challenging. However, the present result can be used to envision some of the useful properties of this vertex for calculations of photon yields and v_2 in a kinematical region that does not restrict the photon energy to be small compared with the field strength. For this purpose we have computed the sum of the squared amplitudes obtained when projecting the explicit computation onto the simple basis of Eq. (8). The squared amplitude shows some of the features that are to be expected, namely, a dominance of photon emission along the production plane (plane transverse to the direction of the magnetic field) and a slightly larger contribution from smaller field strengths for large photon energies. Possible improvements include accounting for the contribution coming from the three loop quarks occupying the lowest and first-excited Landau levels such that, still working in the large field limit, a more complete description can be achieved when the photon energy increases. This is work for the future that will be reported elsewhere.

ACKNOWLEDGMENTS

This work was supported by UNAM-PAPIIT IG100322 and by Consejo Nacional de Ciencia y Tecnología Grants No. A1-S-7655 and No. A1-S-16215. J.D.C.-Y. acknowledges support from Consejo Nacional de Ciencia y Tecnología Grant No. A1-S-7655 in the initial

stages of this work. R.Z. acknowledges support from ANID/CONICYT FONDECYT Regular (Chile) under Grant No. 1200483. A.J.M acknowledges support from FAPESP under Grant No. 2016/12705-7. M.E.T.-Y. acknowledges support by the Simons Foundation through the Simons Foundation Emmy Noether Fellows Program at Perimeter Institute and is grateful for the hospitality of Perimeter Institute where part of this work was carried out. Research at Perimeter Institute is supported in part by the Government of Canada through the Department of Innovation, Science and Economic

Development Canada and by the Province of Ontario through the Ministry of Economic Development, Job Creation and Trade.

APPENDIX A: CALCULATION OF THE TENSORS $D_i^{\mu\nu\alpha}$

The tensors $D_i^{\mu\nu\alpha}$ are obtained by replacing the propagators of Eqs. (21) and (22) into Eq. (18), so that after integration over the coordinate space, they take the form

$$D_1^{\mu\nu\alpha} = \frac{2iq_f g^2}{\pi^2 |q_f B|^2} \int \frac{d^4 r}{(2\pi)^4} \frac{d^4 s}{(2\pi)^4} \frac{d^4 t}{(2\pi)^4} \delta^{(2)}(k_{\parallel} + t_{\parallel} - r_{\parallel}) \delta^{(2)}(s_{\parallel} - p_{\parallel} - r_{\parallel}) \exp\left(-\frac{r_{\perp}^2 + s_{\perp}^2 + t_{\perp}^2}{|q_f B|}\right) \\ \times \exp\left[\frac{2i}{|q_f B|} \epsilon_{mj}(p+r-s)_m(r-t-k)_j\right] \frac{\text{Tr}[\gamma^1 \gamma^2 \gamma_{\perp}^{\mu} \not{t}_{\parallel} \gamma_{\perp}^{\nu} \not{s}_{\parallel} \gamma^{\alpha} \not{s}_{\parallel}] - 2\text{Tr}[\gamma^1 \gamma^2 \gamma_{\parallel}^{\alpha} \not{s}_{\parallel} \gamma^{\mu} \not{t}_{\perp} \gamma^{\nu} \not{t}_{\parallel}]}{(s_{\parallel}^2 - m_f^2 + i\epsilon)(t_{\parallel}^2 - m_f^2 + i\epsilon)(r_{\parallel}^2 - 2|q_f B| - m_f^2 + i\epsilon)}, \quad (\text{A1})$$

$$D_2^{\mu\nu\alpha} = \frac{2iq_f g^2}{\pi^2 |q_f B|^2} \int \frac{d^4 r}{(2\pi)^4} \frac{d^4 s}{(2\pi)^4} \frac{d^4 t}{(2\pi)^4} \delta^{(2)}(k_{\parallel} + t_{\parallel} - r_{\parallel}) \delta^{(2)}(s_{\parallel} - p_{\parallel} - r_{\parallel}) \exp\left(-\frac{r_{\perp}^2 + s_{\perp}^2 + t_{\perp}^2}{|q_f B|}\right) \\ \times \exp\left[\frac{2i}{|q_f B|} \epsilon_{mj}(p+r-s)_m(r-t-k)_j\right] \frac{\text{Tr}[\gamma^1 \gamma^2 \gamma_{\parallel}^{\alpha} \not{s}_{\parallel} \gamma_{\perp}^{\mu} \not{t}_{\parallel} \gamma^{\nu} \not{t}_{\parallel}] - 2\text{Tr}[\gamma^1 \gamma^2 \gamma_{\parallel}^{\nu} \not{t}_{\parallel} \gamma^{\alpha} \not{s}_{\perp} \gamma^{\mu} \not{t}_{\parallel}]}{(r_{\parallel}^2 - m_f^2 + i\epsilon)(t_{\parallel}^2 - m_f^2 + i\epsilon)(s_{\parallel}^2 - 2|q_f B| - m_f^2 + i\epsilon)}, \quad (\text{A2})$$

$$D_3^{\mu\nu\alpha} = \frac{2iq_f g^2}{\pi^2 |q_f B|^2} \int \frac{d^4 r}{(2\pi)^4} \frac{d^4 s}{(2\pi)^4} \frac{d^4 t}{(2\pi)^4} \delta^{(2)}(k_{\parallel} + t_{\parallel} - r_{\parallel}) \delta^{(2)}(s_{\parallel} - p_{\parallel} - r_{\parallel}) \exp\left(-\frac{r_{\perp}^2 + s_{\perp}^2 + t_{\perp}^2}{|q_f B|}\right) \\ \times \exp\left[\frac{2i}{|q_f B|} \epsilon_{mj}(p+r-s)_m(r-t-k)_j\right] \frac{\text{Tr}[\gamma^1 \gamma^2 \gamma_{\perp}^{\nu} \not{t}_{\parallel} \gamma_{\perp}^{\alpha} \not{s}_{\parallel} \gamma^{\mu} \not{t}_{\parallel}] - 2\text{Tr}[\gamma^1 \gamma^2 \not{s}_{\parallel} \gamma_{\parallel}^{\mu} \not{t}_{\parallel} \gamma^{\nu} \not{t}_{\perp} \gamma^{\alpha}]}{(r_{\parallel}^2 - m_f^2 + i\epsilon)(s_{\parallel}^2 - m_f^2 + i\epsilon)(t_{\parallel}^2 - 2|q_f B| - m_f^2 + i\epsilon)}. \quad (\text{A3})$$

The integration over the parallel momenta can be reduced to a single integral provided by the Dirac δ functions, so that

$$r_{\parallel} = t_{\parallel} + k_{\parallel}, \\ s_{\parallel} = t_{\parallel} + q_{\parallel}. \quad (\text{A4})$$

On the other hand, the integration over the perpendicular momenta can be performed by completing the square in the exponentials which leads to three Gaussian integrals over \tilde{r}_{\perp} , \tilde{s}_{\perp} , and \tilde{t}_{\perp} . The latter implies the shifts over the transverse variables within the traces, given by

$$t_j = \tilde{t}_j - i\epsilon_{lj} \left(\frac{1}{2} \tilde{r}_l + \frac{i}{2} \epsilon_{lm} \tilde{r}_m - \tilde{s}_l \right) - A_j, \quad (\text{A5a})$$

$$s_j = \tilde{s}_j - \frac{1}{2} (i\epsilon_{jl} \tilde{r}_l - \tilde{r}_j) - B_j, \quad (\text{A5b})$$

$$r_j = \tilde{r}_j - \frac{1}{4} C_j, \quad (\text{A5c})$$

where

$$A_j = i\epsilon_{lj} \left(B_l - \frac{1}{4} C_l \right), \quad (\text{A6a})$$

$$B_j = \frac{1}{2} \left[\frac{1}{4} C_j - p_j - i\epsilon_{jl} \left(k_l - \frac{1}{4} C_l \right) \right], \quad (\text{A6b})$$

$$C_j = p_j - k_j + i\epsilon_{jl} (p+k)_l. \quad (\text{A6c})$$

Note that the linear terms in the transverse tilde variables vanishes.

For the parallel integration, we perform a Feynman parametrization over the denominators of the tensors $D_i^{\mu\nu\alpha}$. For example, the denominator of the tensor $D_1^{\mu\nu\alpha}$ can be written as

$$d_1 = \frac{1}{(s_{\parallel}^2 - m_f^2 + i\epsilon)(t_{\parallel}^2 - m_f^2 + i\epsilon)(r_{\parallel}^2 - 2|q_f B| - m_f^2 + i\epsilon)} \\ = \int_0^1 dx \int_0^1 dy \int_0^1 dz \frac{2\delta(x+y+z-1)}{\text{den}_1^3}, \quad (\text{A7})$$

where

$$\text{den}_1 = x(s_{\parallel}^2 - m_f^2 + i\epsilon) + y(t_{\parallel}^2 - m_f^2 + i\epsilon) \\ + z(r_{\parallel}^2 - 2|q_f B| - m_f^2 + i\epsilon). \quad (\text{A8})$$

Applying the momentum conservation of Eq. (A4):

$$\text{den}_1 = x[(t_{\parallel} + q_{\parallel})^2 - m_f^2 + i\epsilon] + y(t_{\parallel}^2 - m_f^2 + i\epsilon) \\ + [(t_{\parallel} + k_{\parallel})^2 - 2|q_f B| - m_f^2 + i\epsilon] \\ = \ell_{\parallel}^2 - \Delta_1 + i\epsilon, \quad (\text{A9})$$

with

$$\ell_{\parallel} = t_{\parallel} + xq_{\parallel} + zk_{\parallel} \equiv t_{\parallel} + Q_{\parallel}, \quad (\text{A10})$$

and $\Delta_1(x, y)$ is defined in Eq. (29c). The tensor $D_1^{\mu\nu\alpha}$ splits into two components, correspondent to each trace, namely,

$$D_1^{\mu\nu\alpha} = D_{1(a)}^{\mu\nu\alpha} + D_{1(b)}^{\mu\nu\alpha}, \quad (\text{A11})$$

so that after eliminating odd powers of ℓ_{\parallel} :

$$D_{1(a)}^{\mu\nu\alpha} = \frac{4(2\pi)^5 i q_f g^2}{|q_f B|} e^{f(p_{\perp}, k_{\perp})} \epsilon_{ij} g_{\perp}^{i\mu} g_{\perp}^{j\nu} \int_0^1 dx \int_0^{1-x} dy \int \frac{d^2 \ell_{\parallel}}{(2\pi)^2} \frac{1}{[\ell_{\parallel}^2 - \Delta_1(x, y) + i\epsilon]^3} \\ \times \{ (q_{\parallel}^{\alpha} - Q_{\parallel}^{\alpha} - k_{\parallel}^{\alpha} + Q_{\parallel}^{\alpha} - Q_{\parallel}^{\alpha}) \ell_{\parallel}^2 + (k_{\parallel} - 2Q_{\parallel} - q_{\parallel} + 2Q_{\parallel} + k_{\parallel} + q_{\parallel} - 2Q_{\parallel}) \cdot \ell_{\parallel} \ell_{\parallel}^{\alpha} \\ + (Q_{\parallel}^2 - k_{\parallel} \cdot Q_{\parallel}) (q_{\parallel}^{\alpha} - Q_{\parallel}^{\alpha}) - (Q_{\parallel}^2 - q_{\parallel} \cdot Q_{\parallel}) (k_{\parallel}^{\alpha} - Q_{\parallel}^{\alpha}) - [(q_{\parallel} - Q_{\parallel}) \cdot k_{\parallel} - q_{\parallel} \cdot Q_{\parallel} + Q_{\parallel}^2] Q_{\parallel}^{\alpha} \}, \quad (\text{A12})$$

and

$$D_{1(b)}^{\mu\nu\alpha} = -\frac{2(2\pi)^5 i q_f g^2}{|q_f B|} e^{f(p_{\perp}, k_{\perp})} \epsilon_{ij} C^i \int_0^1 dx \int_0^{1-x} dy \int \frac{d^2 \ell_{\parallel}}{(2\pi)^2} \frac{1}{[\ell_{\parallel}^2 - \Delta_1(x, y) + i\epsilon]^3} \\ \times \{ g_{\perp}^{b\nu} [2\ell_{\parallel}^{\mu} \ell_{\parallel}^{\alpha} - Q_{\parallel}^{\mu} (q_{\parallel}^{\alpha} - Q_{\parallel}^{\alpha}) - Q_{\parallel}^{\alpha} (q_{\parallel}^{\mu} - Q_{\parallel}^{\mu}) - \ell_{\parallel}^2 g_{\parallel}^{\alpha\mu} - (Q_{\parallel}^2 - q_{\parallel} \cdot Q_{\parallel}) g_{\parallel}^{\alpha\mu}] \\ - g_{\perp}^{b\mu} [2\ell_{\parallel}^{\nu} \ell_{\parallel}^{\alpha} - Q_{\parallel}^{\nu} (q_{\parallel}^{\alpha} - Q_{\parallel}^{\alpha}) - Q_{\parallel}^{\alpha} (q_{\parallel}^{\nu} - Q_{\parallel}^{\nu}) - \ell_{\parallel}^2 g_{\parallel}^{\alpha\nu} - (Q_{\parallel}^2 - q_{\parallel} \cdot Q_{\parallel}) g_{\parallel}^{\alpha\nu}] \}. \quad (\text{A13})$$

The integration over ℓ_{\parallel} yields

$$D_{1(a)}^{\mu\nu\alpha} = \frac{4\pi^4 q_f g^2}{|q_f B|} e^{f(p_{\perp}, k_{\perp})} \epsilon_{ij} g_{\perp}^{i\mu} g_{\perp}^{j\nu} \int_0^1 dx \int_0^{1-x} dy \left(\frac{1}{\Delta_1} \right)^2 \\ \times \{ (2Q_{\parallel}^{\alpha} - q_{\parallel}^{\alpha}) \Delta_1 + (Q_{\parallel}^2 - k_{\parallel} \cdot Q_{\parallel}) p_{\parallel}^{\alpha} + (p_{\parallel} \cdot Q_{\parallel}) k_{\parallel}^{\alpha} - [Q_{\parallel}^2 + (q_{\parallel} - 2Q_{\parallel}) \cdot k_{\parallel}] Q_{\parallel}^{\alpha} \}, \quad (\text{A14})$$

and

$$D_{1(b)}^{\mu\nu\alpha} = -\frac{8\pi^4 q_f g^2}{|q_f B|} e^{f(p_{\perp}, k_{\perp})} \epsilon_{ij} C^i \int_0^1 dx \int_0^{1-x} dy \left(\frac{1}{\Delta_1} \right)^2 \\ \times \{ g_{\perp}^{j\nu} [(q_{\parallel} \cdot Q_{\parallel} - Q_{\parallel}^2) g_{\parallel}^{\alpha\mu} - (Q_{\parallel}^{\mu} (q_{\parallel}^{\alpha} - Q_{\parallel}^{\alpha}) + Q_{\parallel}^{\alpha} (q_{\parallel}^{\mu} - Q_{\parallel}^{\mu}))] \\ - g_{\perp}^{j\mu} [(q_{\parallel} \cdot Q_{\parallel} - Q_{\parallel}^2) g_{\parallel}^{\alpha\nu} - (Q_{\parallel}^{\nu} (q_{\parallel}^{\alpha} - Q_{\parallel}^{\alpha}) + Q_{\parallel}^{\alpha} (q_{\parallel}^{\nu} - Q_{\parallel}^{\nu}))] \}. \quad (\text{A15})$$

Implementing that for on-shell propagation, the four-momenta are parallel, namely, Eqs. (6), the above structures can be written as

$$D_1^{\mu\nu\alpha} = C_{(a)}(q) \epsilon_{ij} g_{\perp}^{i\mu} g_{\perp}^{j\nu} q_{\parallel}^{\alpha} + C_{(b)}(q) \epsilon_{ij} q^i [g_{\perp}^{j\nu} (g_{\parallel}^{\mu\alpha} + \Pi_{\parallel}^{\mu\alpha}) - g_{\perp}^{j\mu} (g_{\parallel}^{\nu\alpha} + \Pi_{\parallel}^{\nu\alpha})]. \quad (\text{A16})$$

APPENDIX B: CALCULATIONS OF THE VERTEX COEFFICIENTS $\Gamma_n(\omega_q, \omega_k, q^2)$

We calculate $\Gamma_n(\omega_q, \omega_k, q^2)$ for $n = 1, 2, 3$ in Eq. (8) by projecting Eq. (23) onto the basis

$$\{ v_{\perp}^{\mu} \Pi_{\parallel}^{\nu\alpha}, v_{\perp}^{\nu} \Pi_{\parallel}^{\mu\alpha}, v_{\perp}^{\alpha} \Pi_{\parallel}^{\mu\nu} \}, \quad (\text{B1})$$

where we have used both the transverse polarization vector and the longitudinal polarization tensor as defined in Eqs. (9) and (10). For each of the three $D_i^{\mu\nu\alpha}$ structures in Eq. (23), we get the following set of results:

$$v_{\perp}^{\mu} \Pi_{\parallel}^{\nu\alpha} D_{\mu\nu\alpha}^1 = \frac{8\pi^4 q_f g^2}{|q_f B|} q_{\parallel}^2 e^{f(p_{\perp}, k_{\perp})} |q_{\perp}| \tilde{C} \mathcal{I}_1, \\ v_{\perp}^{\nu} \Pi_{\parallel}^{\mu\alpha} D_{\mu\nu\alpha}^1 = -\frac{8\pi^4 q_f g^2}{|q_f B|} q_{\parallel}^2 e^{f(p_{\perp}, k_{\perp})} |q_{\perp}| \tilde{C} \mathcal{I}_1, \\ v_{\perp}^{\alpha} \Pi_{\parallel}^{\mu\nu} D_{\mu\nu\alpha}^1 = 0, \\ v_{\perp}^{\mu} \Pi_{\parallel}^{\nu\alpha} D_{\mu\nu\alpha}^2 = -\frac{8\pi^4 q_f g^2}{|q_f B|} q_{\parallel}^2 e^{f(p_{\perp}, k_{\perp})} |q_{\perp}| \tilde{B} \mathcal{I}_2, \\ v_{\perp}^{\nu} \Pi_{\parallel}^{\mu\alpha} D_{\mu\nu\alpha}^2 = 0, \quad (\text{B2})$$

$$v_{\perp}^{\alpha} \Pi_{\parallel}^{\mu\nu} D_{\mu\nu\alpha}^2 = \frac{8\pi^4 q_f g^2}{|q_f B|} q_{\parallel}^2 e^{f(p_{\perp}, k_{\perp})} |q_{\perp}| \tilde{B} \mathcal{I}_2, \quad (\text{B3})$$

$$v_{\perp}^{\mu} \Pi_{\parallel}^{\nu\alpha} D_{\mu\nu\alpha}^3 = 0,$$

$$v_{\perp}^{\nu} \Pi_{\parallel}^{\mu\alpha} D_{\mu\nu\alpha}^3 = \frac{8\pi^4 q_f g^2}{|q_f B|} q_{\parallel}^2 e^{f(p_{\perp}, k_{\perp})} |q_{\perp}| \tilde{A}_2 \mathcal{I}_3,$$

$$v_{\perp}^{\alpha} \Pi_{\parallel}^{\mu\nu} D_{\mu\nu\alpha}^3 = -\frac{8\pi^4 q_f g^2}{|q_f B|} q_{\parallel}^2 e^{f(p_{\perp}, k_{\perp})} |q_{\perp}| \tilde{A}_2 \mathcal{I}_3. \quad (\text{B4})$$

Using these results, we can go back to Eq. (8) and collect the contributions that correspond to each coefficient $\Gamma_n(\omega_q, \omega_k, q^2)$. The projection with $v_{\perp}^{\mu} \Pi_{\parallel}^{\nu\alpha}$ from the three sets in (B2)–(B4), contributes to

$$\Gamma_1 = \frac{8\pi^4 q_f g^2}{|q_f B|} e^{f(p_{\perp}, k_{\perp})} |q_{\perp}| q_{\parallel}^2 (\tilde{C} \mathcal{I}_1 - \tilde{B} \mathcal{I}_2) \\ \equiv \frac{8\pi^4 q_f g^2}{|q_f B|} e^{f(p_{\perp}, k_{\perp})} |q_{\perp}| \tilde{\Gamma}_1(\omega_p, \omega_q, \theta). \quad (\text{B5})$$

The projection with $v_{\perp}^{\nu} \Pi_{\parallel}^{\mu\alpha}$ from the three sets in Eqs. (B2)–(B4), contributes to

$$\begin{aligned} \Gamma_2 &= \frac{8\pi^4 q_f g^2}{|q_f B|} e^{f(p_{\perp}, k_{\perp})} |q_{\perp}| q_{\parallel}^2 (\tilde{A}_2 \mathcal{I}_3 - \tilde{C} \mathcal{I}_1) \\ &\equiv \frac{8\pi^4 q_f g^2}{|q_f B|} e^{f(p_{\perp}, k_{\perp})} |q_{\perp}| \tilde{\Gamma}_2(\omega_p, \omega_q, \theta), \end{aligned} \quad (\text{B6})$$

and similarly for the projection with $v_{\perp}^{\alpha} \Pi_{\parallel}^{\mu\nu}$, which contributes to

$$\begin{aligned} \Gamma_3 &= \frac{8\pi^4 q_f g^2}{|q_f B|} e^{f(p_{\perp}, k_{\perp})} |q_{\perp}| q_{\parallel}^2 (\tilde{B} \mathcal{I}_2 - \tilde{A}_2 \mathcal{I}_3) \\ &\equiv \frac{8\pi^4 q_f g^2}{|q_f B|} e^{f(p_{\perp}, k_{\perp})} |q_{\perp}| \tilde{\Gamma}_3(\omega_p, \omega_q, \theta). \end{aligned} \quad (\text{B7})$$

-
- [1] A. Adare *et al.* (PHENIX Collaboration), Observation of Direct-Photon Collective Flow in $\sqrt{s_{NN}} = 200$ GeV Au + Au Collisions, *Phys. Rev. Lett.* **109**, 122302 (2012).
- [2] S. Acharya *et al.* (ALICE Collaboration), Direct photon elliptic flow in Pb-Pb collisions at $\sqrt{s_{NN}} = 2.76$ TeV, *Phys. Lett. B* **789**, 308 (2019).
- [3] A. Adare *et al.* (PHENIX Collaboration), Azimuthally anisotropic emission of low-momentum direct photons in Au + Au collisions at $\sqrt{s_{NN}} = 200$ GeV, *Phys. Rev. C* **94**, 064901 (2016).
- [4] G. David, Direct real photons in relativistic heavy ion collisions, *Rep. Prog. Phys.* **83**, 046301 (2020).
- [5] A. Adare *et al.* (PHENIX Collaboration), Centrality dependence of low-momentum direct-photon production in Au + Au collisions at $\sqrt{s_{NN}} = 200$ GeV, *Phys. Rev. C* **91**, 064904 (2015).
- [6] A. Adare *et al.* (PHENIX Collaboration), Low-momentum direct photon measurement in Cu + Cu collisions at $\sqrt{s_{NN}} = 200$ GeV, *Phys. Rev. C* **98**, 054902 (2018).
- [7] L. Adamczyk *et al.* (STAR Collaboration), Direct virtual photon production in Au + Au collisions at $\sqrt{s_{NN}} = 200$ GeV, *Phys. Lett. B* **770**, 451 (2017).
- [8] J. Adam *et al.* (ALICE Collaborations), Direct photon production in Pb-Pb collisions at $\sqrt{s_{NN}} = 2.76$ TeV, *Phys. Lett. B* **754**, 235 (2016).
- [9] J.-F. Paquet, C. Shen, G. S. Denicol, M. Luzum, B. Schenke, S. Jeon, and C. Gale, Production of photons in relativistic heavy-ion collisions, *Phys. Rev. C* **93**, 044906 (2016).
- [10] C. Gale, J.-F. Paquet, B. Schenke, and C. Shen, Multimesenger heavy-ion collision physics, *Phys. Rev. C* **105**, 014909 (2022).
- [11] H. van Hees, M. He, and R. Rapp, Pseudo-critical enhancement of thermal photons in relativistic heavy-ion collisions? *Nucl. Phys. A* **933**, 256 (2015).
- [12] V. Abgaryan, R. Acevedo Kado, S. V. Afanasyev *et al.*, Status and initial physics performance studies of the MPD experiment at NICA, *Eur. Phys. J. A* **58**, 140 (2022).
- [13] A. Monnai, Direct photons in hydrodynamic modeling of relativistic nuclear collisions, *Int. J. Mod. Phys. A* **37**, 2230006 (2022).
- [14] J. Churchill, L. Yan, S. Jeon, and C. Gale, Emission of electromagnetic radiation from the early stages of relativistic heavy-ion collisions, *Phys. Rev. C* **103**, 024904 (2021).
- [15] A. Kurkela, A. Mazeliauskas, J.-F. Paquet, S. Schlichting, and D. Teaney, Effective kinetic description of event-by-event pre-equilibrium dynamics in high-energy heavy-ion collisions, *Phys. Rev. C* **99**, 034910 (2019).
- [16] A. Kurkela, A. Mazeliauskas, J.-F. Paquet, S. Schlichting, and D. Teaney, Matching the Nonequilibrium Initial Stage of Heavy Ion Collisions to Hydrodynamics with QCD Kinetic Theory, *Phys. Rev. Lett.* **122**, 122302 (2019).
- [17] L. McLerran and B. Schenke, The glasma, photons and the implications of anisotropy, *Nucl. Phys. A* **929**, 71 (2014).
- [18] B. S. Kasmaei and M. Strickland, Photon production and elliptic flow from a momentum-anisotropic quark-gluon plasma, *Phys. Rev. D* **102**, 014037 (2020).
- [19] K. Tuchin, Role of magnetic field in photon excess in heavy ion collisions, *Phys. Rev. C* **91**, 014902 (2015).
- [20] B. G. Zakharov, Effect of magnetic field on the photon radiation from quark-gluon plasma in heavy ion collisions, *Eur. Phys. J. C* **76**, 609 (2016).
- [21] X. Wang, I. A. Shovkovy, L. Yu, and M. Huang, Ellipticity of photon emission from strongly magnetized hot QCD plasma, *Phys. Rev. D* **102**, 076010 (2020).
- [22] X. Wang and I. Shovkovy, Polarization tensor of magnetized quark-gluon plasma at nonzero baryon density, *Eur. Phys. J. C* **81**, 901 (2021).
- [23] N. Sadooghi and F. Taghinavaz, Dilepton production rate in a hot and magnetized quark-gluon plasma, *Ann. Phys. (NY)* **376**, 218 (2017).
- [24] X. Wang and I. A. Shovkovy, Rate and ellipticity of dilepton production in a magnetized quark-gluon plasma, *Phys. Rev. D* **106**, 036014 (2022).
- [25] G. Basar, D. Kharzeev, D. Kharzeev, and V. Skokov, Conformal Anomaly as a Source of Soft Photons in Heavy Ion Collisions, *Phys. Rev. Lett.* **109**, 202303 (2012).
- [26] G. Basar, D. E. Kharzeev, and E. V. Shuryak, Magneto-sonoluminescence and its signatures in photon and dilepton production in relativistic heavy ion collisions, *Phys. Rev. C* **90**, 014905 (2014).
- [27] D. Ávila, F. Nettel, and L. Patiño, Darker and brighter branes, suppression and enhancement of photon production in a strongly coupled magnetized plasma, [arXiv:2204.00024](https://arxiv.org/abs/2204.00024).
- [28] G. Arciniega, F. Nettel, P. Ortega, and L. Patiño, Brighter branes, enhancement of photon production by strong magnetic fields in the gauge/gravity correspondence, *J. High Energy Phys.* **04** (2014) 192.
- [29] Kiminad A. Mamo, Enhanced thermal photon and dilepton production in strongly coupled $N = 4$ SYM plasma in strong magnetic field, *J. High Energy Phys.* **08** (2013) 083.
- [30] S.-Y. Wu and D.-L. Yang, Holographic photon production with magnetic field in anisotropic plasmas, *J. High Energy Phys.* **08** (2013) 032.
- [31] D. E. Kharzeev, L. D. McLerran, and H. J. Warringa, The effects of topological charge change in heavy ion collisions: “Event by event P and CP violation,” *Nucl. Phys. A* **803**, 227 (2008).

- [32] V. Skokov, A. Yu. Illarionov, and V. Toneev, Estimate of the magnetic field strength in heavy-ion collisions, *Int. J. Mod. Phys. A* **24**, 5925 (2009).
- [33] V. Voronyuk, V. D. Toneev, W. Cassing, E. L. Bratkovskaya, V. P. Konchakovski, and S. A. Voloshin, (Electro-)Magnetic field evolution in relativistic heavy-ion collisions, *Phys. Rev. C* **83**, 054911 (2011).
- [34] L. McLerran and V. Skokov, Comments about the electromagnetic field in heavy-ion collisions, *Nucl. Phys. A* **929**, 184 (2014).
- [35] A. Bzdak and V. Skokov, Event-by-event fluctuations of magnetic and electric fields in heavy ion collisions, *Phys. Lett. B* **710**, 171 (2012).
- [36] Z. Wang, J. Zhao, C. Greiner, Z. Xu, and P. Zhuang, Incomplete electromagnetic response of hot QCD matter, *Phys. Rev. C* **105**, L041901 (2022).
- [37] I. A. Shovkovy, Electromagnetic response in an expanding quark-gluon plasma, *Particles* **5**, 442 (2022).
- [38] J. Adam *et al.* (STAR Collaboration), Measurement of e^+e^- Momentum and Angular Distributions from Linearly Polarized Photon Collisions, *Phys. Rev. Lett.* **127**, 052302 (2021).
- [39] J. D. Brandenburg, W. Zha, and Z. Xu, Mapping the electromagnetic fields of heavy-ion collisions with the Breit-Wheeler process, *Eur. Phys. J. A* **57**, 299 (2021).
- [40] A. Ayala, J. D. Castaño-Yepes, C. A. Dominguez, L. A. Hernández, S. Hernández-Ortiz, and M. E. Tejeda-Yeomans, Prompt photon yield and elliptic flow from gluon fusion induced by magnetic fields in relativistic heavy-ion collisions, *Phys. Rev. D* **96**, 014023 (2017); **96**, 119901(E) (2017).
- [41] A. Ayala, J. D. Castaño Yepes, I. Dominguez Jimenez, J. Salinas San Martín, and M. E. Tejeda-Yeomans, Centrality dependence of photon yield and elliptic flow from gluon fusion and splitting induced by magnetic fields in relativistic heavy-ion collisions, *Eur. Phys. J. A* **56**, 53 (2020).
- [42] R. Baier, A. H. Mueller, D. Schiff, and D. T. Son, “Bottom-up” thermalization in heavy ion collisions, *Phys. Lett. B* **502**, 51 (2001).
- [43] O. Garcia-Montero, Non-equilibrium photons from the bottom-up thermalization scenario, *Ann. Phys. (NY)* **443**, 168984 (2022).
- [44] A. Monnai, Prompt, pre-equilibrium, and thermal photons in relativistic nuclear collisions, *J. Phys. G* **47**, 075105 (2020).
- [45] F. Lin and M. Huang, Magnetic correction to the anomalous magnetic moment of electrons, *Commun. Theor. Phys.* **74**, 055202 (2022).
- [46] K. Xu, J. Chao, and M. Huang, Effect of the anomalous magnetic moment of quarks on magnetized QCD matter and meson spectra, *Phys. Rev. D* **103**, 076015 (2021).
- [47] A. Ayala, J. D. Castaño Yepes, M. Loewe, and E. Muñoz, Gluon polarization tensor in a magnetized medium: Analytic approach starting from the sum over Landau levels, *Phys. Rev. D* **101**, 036016 (2020).
- [48] S. L. Adler, J. N. Bahcall, C. G. Callan, and M. N. Rosenbluth, Photon Splitting in a Strong Magnetic Field, *Phys. Rev. Lett.* **25**, 1061 (1970).
- [49] K. Hattori and D. Satow, Gluon spectrum in a quark-gluon plasma under strong magnetic fields, *Phys. Rev. D* **97**, 014023 (2018).
- [50] K. Fukushima, Magnetic-field induced screening effect and collective excitations, *Phys. Rev. D* **83**, 111501(R) (2011).
- [51] A. Ayala, J. D. Castaño Yepes, C. A. Dominguez, S. Hernández-Ortiz, L. A. Hernández, M. Loewe, D. Manreza Paret, and R. Zamora, Thermal corrections to the gluon magnetic Debye mass, *Rev. Mex. Fis.* **66**, 446 (2020).
- [52] A. Ayala, J. L. Hernández, L. A. Hernández, R. L. S. Farias, and R. Zamora, Magnetic corrections to the boson self-coupling and boson-fermion coupling in the linear sigma model with quarks, *Phys. Rev. D* **102**, 114038 (2020).